Available online at www.sciencedirect.com
ScienceDirect
Tetrahedron
Tetrahedron 62 (2006) 11635–11644

Oligomers of β-amino acid bearing non-planar amides form ordered structures

Yuko Otani,[a] Shiroh Futaki,[b,*] Tatsuto Kiwada,[b] Yukio Sugiura,[b] Atsuya Muranaka,[c] Nagao Kobayashi,[c,*] Masanobu Uchiyama,[a] Kentaro Yamaguchi[d] and Tomohiko Ohwada[a,*]

[a]*Graduate School of Pharmaceutical Sciences, The University of Tokyo, 7-3-1 Hongo, Bunkyo-ku, Tokyo 113-0033, Japan*
[b]*Institute for Chemical Research, Kyoto University, Uji, Kyoto 611-0011, Japan*
[c]*Department of Chemistry, Graduate School of Science, Tohoku University, Sendai 980-8578, Japan*
[d]*Faculty of Pharmaceutical Sciences at Kagawa Campus, Tokushima Bunri University 1314-1 Shido, Sanuki, Kagawa 769-2193, Japan*

Received 22 July 2006; revised 19 September 2006; accepted 19 September 2006
Available online 19 October 2006

Abstract—In this report, we explore the feasibility of using bicyclic chiral β-amino acids, (1*R*,2*R*,4*S*)- and (1*S*,2*S*,4*R*)-7-azabicyclo[2.2.1]-heptane-2-carboxylic acid (*R*-**Ah2c** and *S*-**Ah2c**, respectively), to prepare novel peptides with unique properties. Facile *cis–trans* isomerization of the non-planar amide bonds of these β-amino acids should result in great flexibility of the backbone structure of β-peptides containing them. Indeed, oligomers of these amino acids showed thermostability and characteristic CD absorptions, which were not concentration-dependent, suggesting that the oligomers remained monomeric. The results indicated the formation of self-organized monomeric structures with chain-length-dependent stabilization. Energy calculations suggested that the peptides can take helical structures in which the energy barriers to cis–trans isomerization are greater for the central amide bonds than for the terminal amides.

1. Introduction

Recently, design of β-peptides, i.e., peptides containing β-amino acids, has been attracting attention because of the feasibility of derivatization with various side chains at either or both of the α- and β-positions.[1,2] This extends the range of peptide scaffolds potentially available for the creation of novel functional molecules and materials. Since β-peptides are not readily susceptible to proteolysis, they are also promising platforms for the design of new pharmaceuticals, including enzyme inhibitors, receptor agonists, and antagonists.[3]

β-Peptides, comprised of β-amino acids, have an extra methylene group along the backbone, compared with natural proteins. This extra methylene group provides more scope for the introduction of functional side chains on the peptide backbone, but simultaneously results in greater flexibility of the peptide backbone. Therefore, in order to create a spatially ordered structure, methods to reduce the flexibility of the peptide backbone, such as introduction of 2-aminocyclohexanecarboxylic acid,[2c] β-prolines[2d] or bulky substituents,[1a] have been employed. Such structures would diminish the loss of entropy of the protein when an ordered structure is formed by enthalpy-driven intramolecular interaction.[4] Amide bonds in a peptide backbone usually take a planar structure, and this structural feature can be considered to compensate, in some respects, for the entropic loss upon the formation of higher-order structures.[1,2] On the other hand, the planar amide structure also restricts the structural design of peptides, because if we could employ a non-planar amide backbone structure, novel high-order structures might be designable.

Bicyclic 7-azabicyclo[2.2.1]heptane amides (Fig. 1a) take intrinsically non-planar structures, i.e., they exhibit nitrogen-pyramidalization and twisting with respect to the N–C(=O) bond, in the solid,[5a] solution,[5c] and gas (computation) phases.[5b,c] The tilt angles (α) of *N*-aroyl-7-azabicyclo[2.2.1]-heptanes range from 26 to 31° in the X-ray crystal structures.[5] Non-planarity of these amides in solution has also been suggested on the basis of the reduction of rotational barriers to the cis–trans isomerization of the amide bonds (see Fig. 4a). These dynamic features of this skeleton have been proposed to stem from: (i) angle strain of the bicyclic ring structure and (ii) 1,3-allylic type strain induced by the repulsion between the bridgehead protons and the amide moiety. The rigid bicyclic ring structure should also be beneficial to diminish the entropic loss if oligomers of these amino acids form higher-order structures. Although employment of

Keywords: Non-planar amide; β-Amino acids; Oligopeptides; Circular dichroism; Ordered structure.
* Corresponding authors. Tel.: +1 81 3 5841 4730; fax: +1 81 3 5841 4735 (T.O.); fax: +81 22 795 7719 (N.K.); fax: +81 774 32 3038 (S.F.); e-mail addresses: ohwada@mol.f.u-tokyo.ac.jp; nagaok@mail.tains.tohoku.ac.jp; futaki@scl.kyoto-u.ac.jp

0040–4020/$ - see front matter © 2006 Elsevier Ltd. All rights reserved.
doi:10.1016/j.tet.2006.09.062

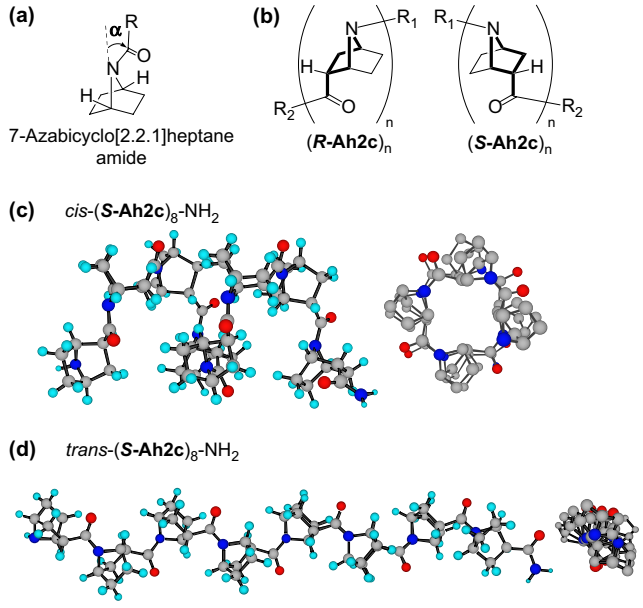

Figure 1. (a) 7-Azabicyclo[2.2.1]heptane amide and (b) **Ah2c** peptides. n=1, 2, 3, 4, 5; R_1=H·HCl, R_2=OH; HCl·H-(*S*-**Ah2c**)$_n$-OH. n=4, 5, 8; R_1=H, R_2=NH_2; H-(*S*-**Ah2c**)$_n$-NH_2. n=8; R_1=H, R_2=NH_2; H-(*R*-**Ah2c**)$_n$-NH_2. Side view and top views of (c) *cis*- and (d) *trans*-H-(*S*-**Ah2c**)$_8$-NH_2 obtained by B3LYP/6-31G* calculations.

such non-planar-amide amino acids is expected to broaden the scope for design of novel peptide-based scaffolds, few studies have been reported on the structures of homo-oligomers with enforced non-planar amides.[6] Thus, in order to obtain basic information about the influence of amide non-planarity on the formation of high-order structures as a step toward the design of functional molecules composed of such amino acids,[7] we have investigated in this study the properties of oligomers of chiral β-amino acids based on the 7-azabicyclo[2.2.1]heptane skeleton, i.e., (1*R*,2*R*,4*S*)-7-azabicyclo[2.2.1]heptane-2-carboxylic acid (*R*-**Ah2c**) and (1*S*,2*S*,4*R*)-7-azabicyclo[2.2.1]heptane-2-carboxylic acid (*S*-**Ah2c**) (Fig. 1b). We show that oligopeptides of our β-amino acids, having enhanced nitrogen inversion and facile *cis–trans* amide isomerization, do form ordered monomeric structures, suggesting the feasibility of employing peptides composed of amino acids bearing non-planar amide bonds as novel peptide scaffolds.

2. Results and discussion

2.1. Synthesis of bicyclic β-amino acids and their homopeptides

Racemic amino acid **5** was synthesized by modifications of the method of Zhang and Trudell,[8] and the enantiomers **6a** and **6b** were each obtained in enantiopure form by repeated recrystallization after introducing Oppolzer's camphorsultam on the carboxylic acid moiety as a chiral auxiliary (Scheme 1).[9]

For the synthesis of the oligomers of this amino acid, the Boc derivatives (**5**-2*R* and 2*S*) and the Fmoc derivatives (**9**-2*R* and 2*S*) were prepared. Since these amino acids have highly hindered and strained structures, we first examined whether construction of oligomers was possible by using solution- and solid-phase methods. Solution-phase synthesis was employed for the preparation of the dimer to pentamer of *S*-**Ah2c**. The benzyl ester of *S*-**Ah2c** was obtained by removing the Boc group from **7**-2*S*, and this was condensed with Boc derivatives of *S*-**Ah2c** (**5**-2*S*) using the hydrochloride

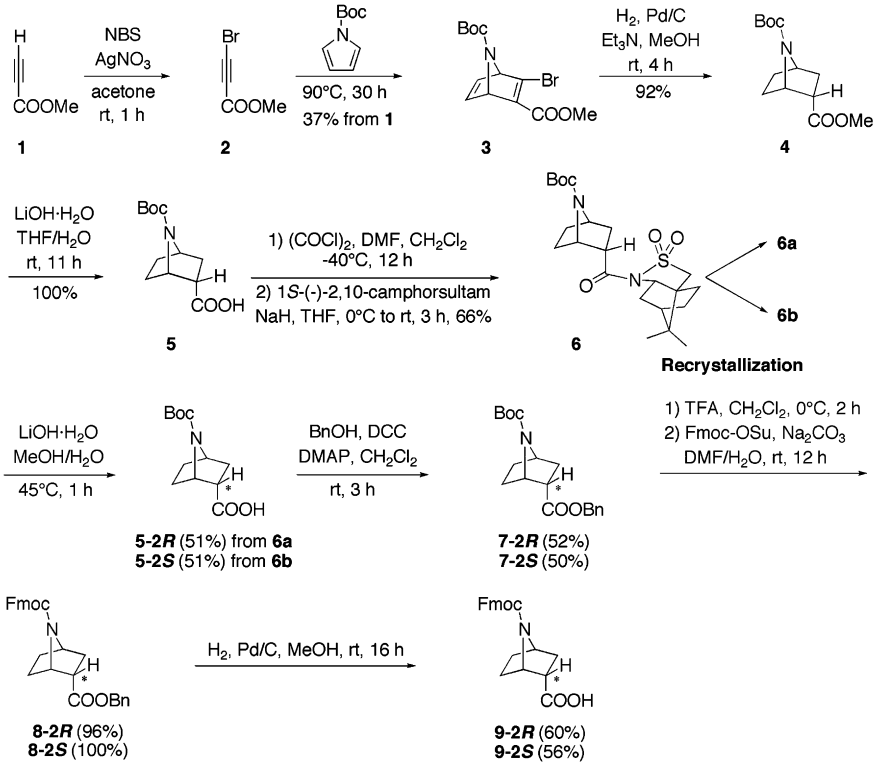

Scheme 1. Synthesis of bicyclic amino acids.

salt of 1-ethyl-3-(3-dimethylaminopropyl)carbodiimide (EDCI·HCl) in DMF (n=2, 3, 4, 5, R_1=*tert*-butoxycarbonyl, R_2=OCH_2Ph). The repetitive removal of the N-terminus of the oligomer and introduction of the Boc derivative of *S*-**Ah2c**, followed by the final deprotection of the N-terminal *tert*-butoxycarbonyl and C-terminal benzyl groups (n=1, 2, 3, 4, 5, R_1=H·HCl, R_2=OH) with catalytic hydrogenation and 4 N HCl treatment, yielded the desired oligomers of *S*-**Ah2c**. Alternatively, solid-phase synthesis using the Rink amide resin and the benzotriazolyloxotris(pyrrolidino)-phosphonium hexafluorophosphate (PyBOP)–*N*-hydroxybenzotriazole (HOBt) coupling procedure was employed for the preparation of the 4-, 5-, and 8-mers of *S*-**Ah2c** (n=4, 5, 8, R_1=H, R_2=NH_2).[9] After construction of the peptide chains, the peptide-resin was treated with trifluoroacetic acid in the presence of ethanedithiol, followed by HPLC purification to give highly pure peptides. The octamer of *R*-**Ah2c** was similarly prepared by the solid-phase procedure (n=8, R_1=H, R_2=NH_2). All syntheses proceeded without difficulty. This suggested that the conventional solution- and solid-phase methods are applicable to this amino acid, in spite of the steric hindrance due to the rigid side chain.

2.2. CD and UV spectroscopic studies of oligomers: chain-length dependence of spectra

In order to study whether the oligomers of *R*-**Ah2c** can generate structure in solution, the circular dichroism (CD) spectra in methanol (100 μM) were recorded. A characteristic and intense CD spectrum of the octamer H-(*R*-**Ah2c**)$_8$-NH_2 was obtained in the far-UV region (190–260 nm) (Fig. 2a). The mean residue ellipticity of H-(*R*-**Ah2c**)$_8$-NH_2 shows a maximum at 198 nm and a minimum at 217 nm. This spectrum does not coincide with those of typical structures of natural peptides (composed of α-amino acids), but resembles those observed for helical β-peptide oligomers based on β-proline[2d] and those of helical β-peptide oligomers with amide protons based on *trans*-2-aminocyclopentanecarboxylic acid[2c] or β^{2,3}-peptide (compound **7c** in Ref. 1a), reported previously.

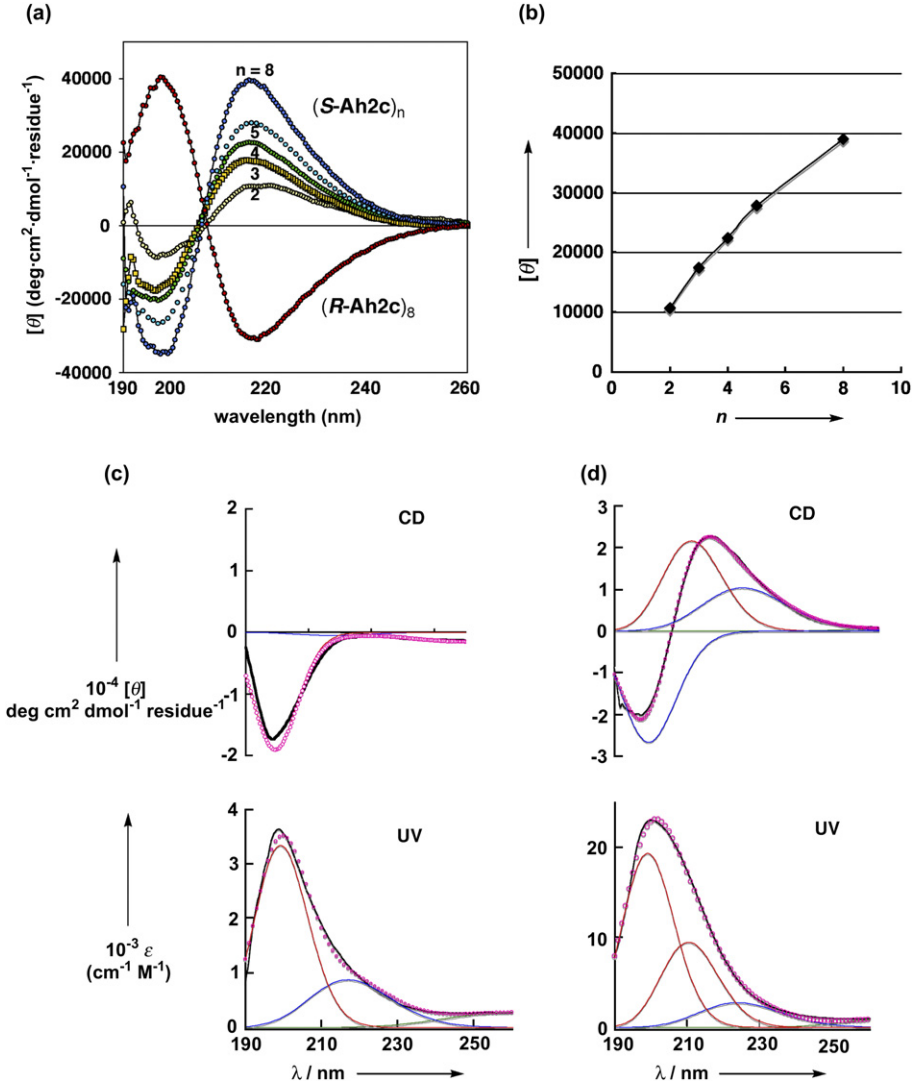

Figure 2. (a) CD spectra of H-(*R*-**Ah2c**)$_8$-NH_2, HCl·H-(*S*-**Ah2c**)$_{1-5}$-OH, and H-(*S*-**Ah2c**)$_8$-NH_2 measured at 100 μM in MeOH at 20 °C. (b) Dependence of CD intensity at 217 nm on the number of oligomers of (*S*-**Ah2c**)$_n$, derived from (a). Band deconvolution of the UV and CD spectra of (c) HCl·H-(*S*-**Ah2c**)-OH (monomer) measured at 100 μM in MeOH and (d) HCl·H-(*S*-**Ah2c**)$_4$-OH (tetramer) measured at 100 μM in MeOH. Sample cells of 1-mm path length were used for CD measurement. Black line: experimental spectra of **Ah2c** monomer or tetramer measured at 100 μM in MeOH at 20 °C (CD) and at rt (UV), red line: π–π* transition, blue line: n–π* transition, pink circles: simulated spectra.

The octamer peptide of the enantiomeric configuration, H-(*S*-**Ah2c**)$_8$-NH$_2$, showed a symmetric spectrum with respect to that of H-(*R*-**Ah2c**)$_8$-NH$_2$ in terms of the Cotton effects. This suggests that, even though these enantiomeric amino acids have flexibility in the amide structure, their oligomers converge in terms of higher-order structures; this suggests the induction of thermodynamically stable conformations. Of particular interest is the observation of an apparent length-dependent trend in the CD spectra of the *S*-**Ah2c** oligomers: in the CD spectra of the trimer, tetramer, pentamer, and octamer of *S*-**Ah2c**, the positions of the minimum (198 nm) and the maximum (217 nm) are similar, and the intensity per residue (values normalized for concentration and the number of residues) at both the minimum and the maximum increase as the number of monomer units increases (Fig. 2b).[10] These oligomers also showed an isodichroic point (see below). This observation strongly suggests that CD-active regular secondary structures are induced and are increasingly favored as the peptide chain is elongated. Note that H-(*S*-**Ah2c**)$_n$-NH$_2$ and H-(*S*-**Ah2c**)$_n$-OH (n=4 and 5) showed practically identical CD spectra in methanol, indicating that the difference in C-terminal structure does not significantly affect the higher-order structure formation. Similar chain-length-dependent increase in CD intensities has also been observed in other ordered systems.[3,10] In the case of water-soluble amphiphilic peptides, aggregation stimulated by hydrophobic interaction would be a cause of such stabilization. However, this is not so in the present case; essentially identical CD spectra were obtained at peptide concentrations in the range of 50–1000 μM for H-(*S*-**Ah2c**)$_5$-NH$_2$ and HCl·H-(*S*-**Ah2c**)$_4$-OH with no significant change in molecular ellipticity at 217 nm ($[\theta]_{217}$) (Fig. 3). Since methanol is effective to reduce hydrophobic interactions, inhibiting possible aggregation of peptides,[11] these results are suggestive of monomeric structures of the oligomers.

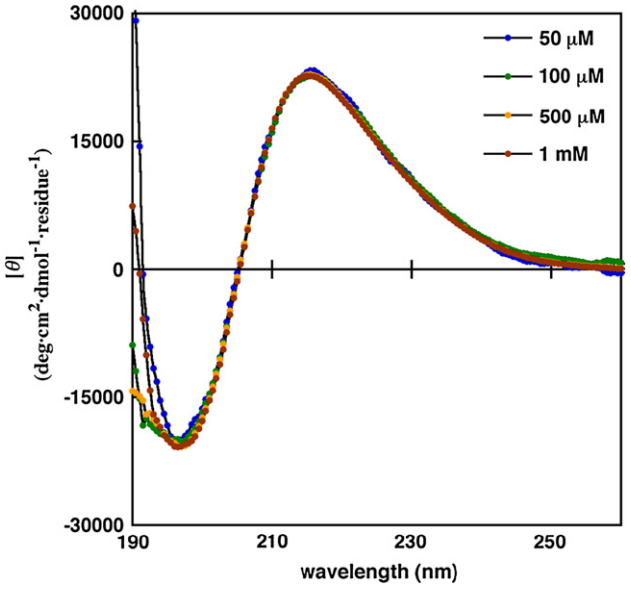

Figure 3. Concentration dependence study. CD spectra of HCl·H-(*S*-**Ah2c**)$_4$-OH at 50, 100, 500, and 1000 μM (1 mM) in MeOH at 20 °C. There is a normal concentration dependency in the intensity of the CD spectra between 50 and 1000 μM in methanol; that is, after concentration normalization, the CD spectra are consistent.

Therefore, the **Ah2c** peptides are considered to adopt a *self-organized* monomeric structure. The question arises, what is the major driving force for the structure formation? In a hydrophobic environment, intramolecular hydrogen bonding or ion-pair interaction is effective. However, this is not the case here, since there is no amide proton or charged group in these peptides; thus, presumably the increase of the inter-residue van der Waals attraction[3,12] is a factor in this structural organization. Support for this interpretation comes from the results of the study of the thermal stability of these peptides. A gradual decrease in $[\theta]_{217}$ in the CD spectra of the octamer, pentamer, and tetramer peptides was observed when the temperature was raised to 60 °C: decreases of 11, 20, and 31% compared with the $[\theta]_{217}$ values at 20 °C were obtained, respectively, and no significant thermal transition of these peptides was observed. The degree of the reduction of $[\theta]_{217}$ is smaller in longer peptides, which suggests stabilization of the secondary structures in longer peptides.

2.3. Structure of the oligomers

The above results suggested that, even when a peptide lacks a planar amide structure and has flexibility in the amide bonds, it can show a preference for ordered structures, presumably with the contribution of conformationally strained side chains to reduce entropic loss upon the thermodynamically driven formation of the high-order structures. NMR study of the tetramer only gave broad signals for all the protons (see Supplementary data, Fig. S3), which is consistent with the presence of a mixture of isomers with respect to the *cis–trans* amides in the oligomers. This possible cis–trans isomerization was confirmed by NMR measurement of the terminal-protected dimer of **Ah2c**; in the ^{1}H NMR spectrum ($CDCl_3$) of the *N*-Boc-*S*-dimer-benzyl ester, a mixture of *cis*- and *trans*-amide (*cis:trans*=47:53) structures with respect to the central amide bond was observed (see Supplementary data, Fig. S2) (the *trans*-amide crystal structure was obtained for *t*-Boc-(*R*-**Ah2c**)$_2$-OBn; Fig. 4 (CCDC 621064), see Supplementary data for a summary of the data). This observed non-biased mixture of the isomers is compatible with the calculated small energy difference (Fig. 5). Thus, there is an equilibrium mixture of *cis*- and *trans*-amide structures in solution. Since the oligomers have several amide bonds, overlapping of the signals from various *cis–trans* isomerization states of the peptide would give broad and complex signals, making structural characterization difficult. However, it is plausible that oligomerization of **Ah2c** may increase the preference for the ultimate, thermodynamically stable ordered structures. This would be consistent with the observed chain-length dependency and thermostability of the peptides.

The possible formation of helical structure was next examined. Firstly, the UV and CD spectra of the oligopeptides were compared with those of the corresponding monomeric amino acid. As shown in Figure 2c, the monomer exhibited an intense absorption band at ca. 200 nm and a shoulder at longer wavelength. As is usual for naturally occurring peptides, these bands can be assigned, respectively, to the electric dipole allowed π–π* transition and the forbidden n–π* transition of the peptide chromophore.[13] The UV absorption bands of the oligomers broadened systematically toward

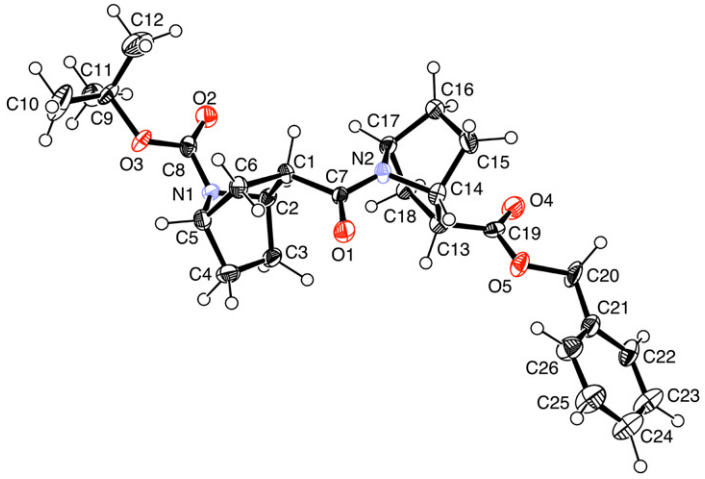

Figure 4. ORTEP diagram of *trans*-amide structure of dimer, *t*-Boc-(*R*-**Ah2c**)$_2$-OBn (at 150 K).

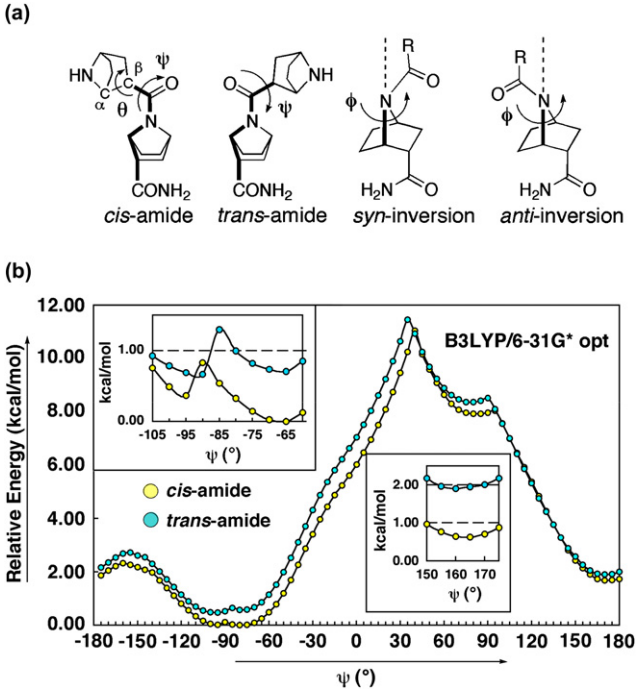

Figure 5. (a) *cis*- and *trans*-Amide dimers, H-(*S*-**Ah2c**)$_2$-OH, of 7-azabicyclo[2.2.1]heptane amide and their *syn*- and *anti*-inversions. (b) Scans of the potential surface at the B3LYP/6-31G* level for the cis- (yellow) and trans-conformers (green). The potential surface was scanned with respect to the ψ torsion for *cis*-H-(*S*-**Ah2c**)$_2$-OH (yellow) and *trans*-H-(*S*-**Ah2c**)$_2$-OH (green). Inset: energies (MP2/6-31G* level) are relative to the global minimum, *cis* (−65°). Two additional minima for *cis*-(*S*-**Ah2c**)$_2$ are located at ψ values of −95° and 165°. Three minima for *trans*-H-(*S*-**Ah2c**)$_2$-OH are located at −90°, −65°, and 160°.

the longer-wavelength region, with increasing number of monomeric units. While the CD signals of the oligopeptides appear to be dispersion-type signals, an absorption-shaped CD signal was observed for the monomeric amino acid.

In order to estimate the number of transitions in the UV region, a band deconvolution analysis of the experimental data was carried out (Fig. 2c and d). This approach rests on the fact that a single set of Gaussian components can be used for fitting of both the UV and CD spectra (Table 1).[14] In the case of the monomer, three Gaussian bands were used, two of which can be associated with the π–π* (red line, λ_{max}=200 nm, f=0.063) (red line) and n–π* (blue line, λ_{max}=218 nm, f=0.022) (blue line) transitions (Fig. 2c). In contrast, at least four Gaussian bands were required to fit the spectra of the tetramer. The two higher-energy bands (λ_{max}=199 nm, f=0.374 and λ_{max}=211 nm, f=0.182) should be associated with the splitting of the π–π* transitions (red line) as a result of the strong exciton interactions, while the lower-energy band (λ_{max}=225 nm, f=0.066) was assigned to the n–π* band (blue line) (Fig. 2d). As a result, the intense CD signals observed for the oligomers are considered to arise from couplings between the n–π* transition and the π–π* transitions on nearby amides,[15] as well as couplings between the π–π* transitions of the amide units,[16] similar to those of α-helical polypeptides. Since these CD signals would depend strongly on the transition moment directions, it can be concluded that the oligomers adopt well-defined structures, plausibly helical structures, under the experimental conditions.

Table 1. Results of the Gaussian fit analysis of the monomer and tetramer

Compound	Band no.	Assignment	Wavelength (nm)	Energy (cm^{-1})	Intensity (dm^3/mol cm)	Bandwidth (cm^{-1})	Oscillator strength (f)	μ (D)
Monomer	1		262	38,140	274	6666	0.008	0.09
	2	n–π*	218	45,970	874	5390	0.022	0.19
	3	π–π*	200	50,121	3332	4103	0.063	0.51
Tetramer	1		271	36,908	1373	5258	0.033	0.37
	2	n–π*	225	44,529	2721	5282	0.066	0.61
	3	π–π*	211	47,454	9475	4169	0.182	1.57
	4	π–π*	199	50,157	19,299	4209	0.374	3.05

2.4. Model study

Assuming that the oligomers prefer helical structures, then what kind of structure is probable? To address this question, quantum chemical calculations were carried out first for the dimer, H-(*S*-**Ah2c**)$_2$-OH, at the B3LYP/6-31G* level. In the case of β-amino acids such as those in this study, there are three valuable parameters.[17] The ϕ, θ, and ψ torsions are defined as [$C_{(i-1)}$–N_i–$C_{\alpha i}$–$C_{\beta i}$], [N_i–$C_{\alpha i}$–$C_{\beta i}$–C_i], and [$C_{\alpha i}$–$C_{\beta i}$–C_i–$N_{(i+1)}$], respectively. In the present case, $\phi=-91^\circ$ (in the case of *syn*) or -151° (in the case of *anti*) and $\theta=-162^\circ$ due to the rigid bicyclic 7-azabicyclo[2.2.1]-heptane structure, so that the most stable structure(s) can be obtained only by changing ψ. We have considered two types of isomerism of amide (*cis* and *trans*) and two directions of inversion (*syn* and *anti*) (Fig. 5a). The ψ value was changed stepwise every five degrees and the obtained structures were optimized. For each ψ, both *syn*- and *anti*-inversion cases were calculated for the *cis*-amide and *trans*-amide structures and the energetically more stable cases with respect to the inversion were chosen (Fig. 5b). A calculated inversion barrier was small (2.5 kcal/mol).[5c] Three energetically minimum structures were obtained for both the *cis*- and *trans*-amide structures. The results indicate that the amide bonds are not planar and that they take *cis*- or *trans*-conformation. Further calculations at the MP2/6-31G* level in the vicinity of the above three minima revealed that the most stable structure is the *cis*-amide at $\psi=-65^\circ$ attained via *syn*-inversion (the most stable *trans*-amide was obtained at $\psi=-90^\circ$ via *syn*-inversion, but the energy is higher than that of the most stable *cis*-amide by 0.69 kcal/mol). The same result was obtained when the solvent (water) was taken into account. The ϕ, θ, and ψ values in the most stable structure, after full optimization, were -86°, -162°, and -65°, respectively.

A single crystal structure of the *trans*-amide of the enantiotropic dimer, *t*-Boc-(*R*-**Ah2c**)$_2$-OBn was obtained (Fig. 4). The central amide bond is pyramidalized ($\alpha=21.5^\circ$), and the nitrogen atom is *syn*-inverted. The observed torsion angles, ψ, ϕ and θ were +82.9 (3)°, +98.3 (3)°, and +153.2 (2)°, respectively. The absolute magnitudes of these values were consistent with the computationally estimated values (-90°, -91°, and -162°, respectively) of the most stable *trans*-amide structure of the *S*-dimers (that is, *syn*-inverted). This supports the validity of the present computational structural analysis.

In the next step, a Monte-Carlo conformation search was performed for the all *cis*- or *trans*-amide forms of the octamer (H-(*S*-**Ah2c**)$_8$-NH_2) by means of MMFF94s force-field calculations, and the resultant most stable structure was further optimized at the B3LYP/6-31G* level. It was found that the *cis*-amide conformer takes a left-handed helical structure with four residues per turn (Fig. 1c), while the *trans*-amide conformer takes an elongated helical structure with roughly two residues per turn (Fig. 1d). The average values of the torsion angle ψ ($C_{\alpha i}$–$C_{\beta i}$–C_i–$N_{(i+1)}$) of the optimized structures of the octamer are -68° for the *cis*-amide helix, and -90° for the *trans*-amide helix. These ψ values are consistent with those for the energy minimum structures of the *cis*- and *trans*-dimers, respectively (Fig. 5). The *cis*-amide helix structure was estimated to be more stable than the *trans*-amide helical structure by 7.8 kcal/mol by means of MP2/6-31G* calculations. This result, together with the presence of an isodichroic point for oligomers with $n=3$–8 (Fig. 2a), allows us to propose a possible ultimate structure of the oligomers of bicyclic β-amino acids with 7-azabicyclo[2.2.1]heptane, i.e., a helical structure with *cis*-amide and with four residues per turn, in the presence of the *trans* conformer to some extent. It was also shown that the energy barriers with respect to the *cis–trans* isomerization increase in the center of the oligomers as compared with the terminal amides in the hexamer (H-(*S*-**Ah2c**)$_6$-NH_2): in the model cis-helix structure of the hexamer (H-(*S*-**Ah2c**)$_6$-NH_2) obtained similarly, the *cis*-to-*trans* rotational barriers were as follows: with respect to the first amide bond from the N-terminal: HF/6-31G*, 10.65 kcal/mol (HF/3-21G*, 9.28 kcal/mol); the second amide bond: HF/6-31G*, 11.32 kcal/mol (HF/3-21G*, 9.08 kcal/mol); the third amide bond: HF/6-31G*: 12.29 kcal/mol (HF/3-21G*:11.52 kcal/mol). The rotational barrier increased toward the center along the helix. This is consistent with the length-dependent increase of the robustness of the ordered structures deduced from the CD spectra.

3. Conclusions

In this study, we have shown that homooligomers of bicyclic β-amino acids containing 7-azabicyclo[2.2.1]heptane **Ah2c**, which lacks amino hydrogen and has a spatially hindered structure, can be synthesized without difficulty. Although coexistence of the *cis* and *trans* isomers with respect to the non-planar amide bonds has been suggested, oligomerization of **Ah2c** significantly promoted the formation of higher-order structures, yielding characteristic CD spectra. Deconvolution and modeling studies suggest the formation of unique helical structures without intramolecular hydrogen bonds. These results support the idea that β-amino acids bearing non-planar amide bonds can be used to generate novel protein scaffolds. The ordered structure may be attained owing to the spatially strained structure of the side chain, which would compensate for the loss of entropy and simultaneously gain enthalpy to form the ordered structures in the presence of cis–trans isomerizable amide bonds. On the other hand, the non-planarity of the amide bond should endow the resulting scaffolds with unique features, which may yield properties different from those of scaffolds composed of units with typical planar amide bonds. The results obtained in this study suggest that it may also be feasible to construct protein scaffolds comprised of other *N*-substituted β-amino acids. Because of the interest in chemical features of amino acid derivatives based on the 7-azabicyclo[2.2.1]-heptanes, the possibility of derivatization at amide nitrogen, in addition to α- and β-carbon atoms, should offer great scope to design novel functional molecules and materials showing unique chemical and physical properties. Thus, we believe our results make feasible a novel approach to protein scaffold design.

4. Experimental

4.1. General methods

All the melting points were measured with a Yanagimoto Micro Melting Point Apparatus and are uncorrected. Proton

(400 MHz) NMR spectra were measured on a JEOL Caliber-GX400 NMR spectrometer with TMS as an internal reference in $CDCl_3$ as the solvent, unless otherwise specified. Chemical shifts δ are shown in parts per million. Coupling constants are given in hertz. Low-resolution EI mass spectra (MS, EI^+) and high-resolution EI mass spectra (HRMS, EI^+) were recorded on a JEOL JMS-O1SG-2 spectrometer. Low-resolution FAB mass spectra (MS, FAB^+) and high-resolution FAB mass spectra (HRMS, FAB^+) were recorded on a JEOL MStation JMS-700 spectrometer. Matrix-assisted laser desorption ionization time-of-flight mass spectra (MALDI-TOF MS) were recorded on an Applied Biosystems Voyager-DE STR instrument. ESI-TOF MS (ESI^+) were recorded on a Bruker Daltonics, micro-TOF-LC, and Micromass, micromass-LCT instruments. Column chromatography was carried out on silica gel (silica gel 60 N (100–210 μm), Merck). The combustion analyses were carried out in the microanalytical laboratory of this faculty.

4.2. Materials

Racemic bicyclic amino acid (**5**) was synthesized by modifications of the method of Zhang and Trudell and Singh et al.,[8,18–20] and each optically pure enantiomer was obtained by repeated recrystallization after introducing Oppolzer's camphorsultam on the carboxylic acid moiety as a chiral auxiliary.

4.3. Synthesis of chiral bicyclic amino acids

4.3.1. Methyl 3-bromopropiolate (2). To a magnetically stirred solution of methyl propionate **1** (25 mL, 281 mmol) in acetone (300 mL) at rt, silver nitrate (4.71 g, 27.7 mmol) was added, followed by the addition of *N*-bromosuccinimide (58.26 g, 327.3 mmol) in one portion. The homogeneous solution turned cloudy within 5 min, then a grayish solid was precipitated and the whole was stirred for 1 h. Acetone was removed carefully under reduced pressure at rt and the residue was distilled at rt to afford **2** as a pale yellow oil (45.2 g as a mixture of acetone, 67% NMR yield).

^{1}H NMR: 3.79 (s, 3H).

4.3.2. Methyl 2-bromo-7-(*tert*-butoxycarbonyl)-7-azabicyclo[2.2.1]hepta-2,5-diene-2-carboxylate (3). A solution of **2** (188 mmol) and *tert*-butyl 1-pyrrolecarboxylate (100 mL, 598 mmol) in acetone was heated at 90 °C for 30 h with stirring under Ar atmosphere. The resulting mixture was subjected to column chromatography (*n*-hexane/AcOEt 9:1). Compound **3** (33.92 g, 37% yield) was obtained as a yellow oil.

^{1}H NMR: 7.13 (br s, 2H), 5.50 (br s, 1H), 5.15 (br s, 1H), 3.79 (s, 3H), 1.41 (s, 9H).

4.3.3. Methyl 7-(*tert*-butoxycarbonyl)-7-azabicyclo-[2.2.1]heptane-2-carboxylate (4). A solution of **3** (367 mg, 1.11 mmol) in MeOH was hydrogenated catalytically (10% Pd/C) in the presence of triethylamine (218 mg, 2.15 mmol). The mixture was filtrated, the solvent was evaporated, and the residue was subjected to column chromatography (*n*-hexane/$CHCl_3$=1/6, then $CHCl_3$ only). Hydrogenated compound **4** (262 mg, 92% yield) was obtained as a yellow oil.

^{1}H NMR: 4.39 (br s, 1H), 4.21 (br s, 1H), 3.70 (s, 3H), 3.04 (m, 1H), 2.00–1.50 (m, 6H), 1.47 (s, 9H).

4.3.4. 7-(*tert*-Butoxycarbonyl)-7-azabicyclo[2.2.1]heptane-2-carboxylic acid (5). To a solution of **4** (7.90 g, 30.95 mmol) in THF (80 mL), a solution of lithium hydroxide monohydrate (1.60 g, 38.13 mmol) in 20 mL of water was added, and the mixture was stirred at rt for 11 h. The organic solvent was evaporated and the residue was acidified to pH=2. Then the whole was extracted with AcOEt, the organic phase was washed with brine, and the solvent was evaporated to afford **5** (7.25 g, quant.) as a brown oil.

MS (*m*/*z*): 241 ($M+H^+$). HRMS (EI^+, $M+H^+$) calcd for $C_{12}H_{19}NO_4$: 241.1313; obsd: 241.1308. ^{1}H NMR: 4.45 (br s, 1H), 4.23 (br s, 1H), 3.13–3.10 (m, 1H), 2.00–1.46 (m, 6H), 1.46 (s, 9H).

4.3.5. 7-(*tert*-Butoxycarbonyl)-2-*endo*-bornane-2,10-sultam-7-azabicyclo[2.2.1]heptane (6). To a stirred solution of **5** (936 mg, 3.79 mmol) in dry CH_2Cl_2 was added dropwise a solution of oxalyl chloride (0.8 mL, 9.1 mmol) in dry CH_2Cl_2 at −70 °C. When the addition was finished, a catalytic amount of dry DMF (two drops) was added, and the reaction mixture was stirred for 24 h at −40 °C. The solvent and unreacted oxalyl chloride were removed in vacuum to afford the acid chloride. Under Ar atmosphere, a solution of 1*S*-(−)-2,10-camphorsultam (1000 mg, 4.64 mmol) in THF was added to a solution of NaH (65% in oil, washed with *n*-hexane, 383 mg, 10.37 mmol) in THF at 0 °C and the reaction mixture was stirred for 20 min at 0 °C. Then to the mixture was added dropwise a solution of the acid chloride in THF at 0 °C and the whole was stirred for 12 h at rt. Addition of water, followed by 2 N aqueous HCl, quenched the reaction, and the whole was extracted with AcOEt, and the organic layer was washed with brine and dried over Na_2SO_4. The solvent was evaporated to give a pale yellow solid, which was chromatographed (*n*-hexane/AcOEt=4/1) to give a mixture of **6a** and **6b** (1.13 g, 66% yield). The mixture was stirred in *n*-hexane/Et_2O/AcOEt to give a suspension and the precipitate was filtered to afford **6b** as a colorless solid. Pure **6a** was obtained as colorless needles by recrystallization of the residue from *n*-hexane/CH_3CN/$^i Pr_2O$.

4.3.5.1. 6a + 6b. Anal. Calcd for $C_{22}H_{34}N_2O_5S$: C, 60.25; H, 7.81; N, 6.39. Found: C, 59.95; H, 7.58; N, 6.32.

Compound **6a**: mp 182.9–183.1 °C (colorless needles). Anal. Calcd for $C_{22}H_{34}N_2O_5S$: C, 60.25; H, 7.81; N, 6.39. Found: C, 60.55; H, 7.86; N, 6.40. ^{1}H NMR: 4.71–4.69 (1H, m), 4.25–4.21 (1H, m), 3.91–3.87 (1H, m), 3.58–3.53 (1H, m), 3.51 (1H, d, *J*=14.0 Hz), 3.46 (1H, d, *J*=14.0 Hz), 2.10–1.63 (13H, m), 1.47 (9H, s), 1.15 (3H, s), 0.98 (3H, s).

Compound **6b**: mp 208.0–208.5 °C (colorless solid). Anal. Calcd for $C_{22}H_{34}N_2O_5S$: C, 60.25; H, 7.81; N, 6.39. Found: C,

60.10; H, 7.76; N, 6.40. ^{1}H NMR: 4.66–4.64 (1H, m), 4.24–4.22 (1H, m), 3.91–3.89 (1H, m), 3.62–3.55 (1H, m), 3.52 (1H, d, J=14.0 Hz), 3.44 (1H, d, J=13.6 Hz), 2.10–1.80 (7H, m), 1.80–1.65 (2H, m), 1.60–1.40 (4H, m), 1.47 (9H, s), 1.15 (3H, s), 0.99 (3H, s).

4.3.6. (1*R*,2*R*,4*S*)-7-(*tert*-Butoxycarbonyl)-7-azabicyclo[2.2.1]heptane-2-carboxylic acid (5-2*R*). A solution of **6a** (2.29 g, 5.21 mmol) in 40 mL of MeOH/H_2O (3:1) mixture containing $LiOH\cdot H_2O$ (220 mg, 5.24 mmol) was warmed to 45 °C with stirring. After 1 h, the mixture was cooled and the resulting solution was extracted with AcOEt to remove the chiral auxiliary sultam. The aqueous layer was acidified to pH=3 with 1 N aqueous HCl under an ice-cold condition, and the whole was extracted with $CHCl_3$. The crude acid **5**-2*R* (641 mg, yield 51%) was obtained as a pale yellow oil after evaporation of the organic solvent.

4.3.7. (1*S*,2*S*,4*R*)-7-(*tert*-Butoxycarbonyl)-7-azabicyclo[2.2.1]heptane-2-carboxylic acid (5-2*S*). Compound **5**-2*S* was obtained in a similar manner to **5**-2*R*, described above.

4.3.8. Determination of the absolute stereochemistry of 5-2*R*. The absolute configuration of the resolved material was established by the optical rotation, and crystallographically.

Carboxylic acid **5**-2*R* (8 mg, 0.033 mmol) was converted to methyl ester by using TMS–diazomethane in benzene. Then the reaction mixture was evaporated to give quantitatively 10 mg of white solid (**4**-2*R*).

$[\alpha]_D^{23}$ −20.80 (*c* 0.50, $CHCl_3$), lit.[20] $[\alpha]_D^{23}$ −22.6 (*c* 1.01, $CHCl_3$).

4.3.9. (1*R*,2*R*,4*S*)-7-(*tert*-Butoxycarbonyl)-7-azabicyclo[2.2.1]heptane-2-carboxylic acid 2-benzyl ester (7-2*R*). To a solution of **5**-2*R* (713 mg, 2.95 mmol), benzyl alcohol (0.95 mL, 9.11 mmol), and dimethylaminopyridine (290 mg, 2.37 mmol) in 5 mL of CH_2Cl_2 was added dicyclohexylcarbodiimide (671 mg, 3.25 mmol) at 0 °C. The whole was warmed to rt and stirred for 3 h. The precipitate was filtered and washed with ether. The combined organic layer was washed with 0.5 N aqueous HCl, saturated aqueous $NaHCO_3$, dried over Na_2SO_4, and the solvent was evaporated. The residue was chromatographed (*n*-hexane/AcOEt=2/1) to give **7**-2*R* as a yellow oil (513 mg, 52% yield).

MS (*m*/*z*): 331 ($M+H^+$). HRMS (EI^+, $M+H^+$) calcd for $C_{19}H_{25}NO_4$: 331.1782; obsd: 331.1797. ^{1}H NMR: 7.40–7.33 (5H, m), 5.14 (2H, s), 4.42–4.40 (1H, m), 4.21–4.19 (1H, m), 3.13–3.06 (1H, m), 1.97–1.91 (1H, m), 1.90–1.85 (1H, m), 1.85–1.80 (1H, m), 1.73–1.67 (1H, m), 1.45 (9H, s), 1.45 (2H, m, overlap).

4.3.10. (1*S*,2*S*,4*R*)-7-(*tert*-Butoxycarbonyl)-7-azabicyclo[2.2.1]heptane-2-carboxylic acid 2-benzyl ester (7-2*S*). Compound **7**-2*S* was obtained in a similar manner to **7**-2*R*, described above.

4.3.11. (1*R*,2*R*,4*S*)-7-(Fluorenylmethyl)-7-azabicyclo[2.2.1]heptane-2,7-dicarboxylic acid 2-benzyl ester (8-2*R*). To a solution of **7**-2*R* (351 mg, 1.06 mmol) in 2 mL of dry CH_2Cl_2 was added 2 mL of trifluoroacetic acid at 0 °C and the mixture was stirred for 1.5 h at 0 °C. Then the solvent was evaporated to give a crude oil. This residue was dissolved in 7 mL of water, and to this solution Na_2CO_3 (320 mg, 3.01 mmol) was added, followed by the addition of a solution of 9-fluorenylmethyl succinimidyl carbonate (471 mg, 1.40 mmol) in 7 mL of dry DMF at 0 °C. The resultant viscous solution was stirred vigorously for 12 h at rt. The aqueous layer was acidified to pH=3 with 1 N aqueous HCl and the whole was extracted with AcOEt. The organic layer was washed with brine, dried over Na_2SO_4, and the solvent was evaporated to give a crude oil, which was chromatographed (*n*-hexane/AcOEt=2/1) to give **8**-2*R* as a red-brown oil (461 mg, 96% yield). MS (*m*/*z*): 453 ($M+H^+$). HRMS (EI^+, $M+H^+$) calcd for $C_{29}H_{27}NO_4$: 453.1939; obsd: 453.1931. ^{1}H NMR: 7.71–7.69 (2H, m), 7.58–7.55 (2H, m), 7.38–7.26 (9H, m), 5.13 (2H, s), 4.49–4.30 (2H, m), 4.38 (1H, br s), 4.19 (2H, t, J=6.2 Hz), 3.00–2.80 (1H, br s), 1.84–1.82 (2H, m), 1.70–1.67 (1H, m), 1.63–1.58 (1H, m), 1.46–1.37 (2H, m).

4.3.12. (1*S*,2*S*,4*R*)-7-(Fluorenylmethyl)-7-azabicyclo[2.2.1]heptane-2,7-dicarboxylic acid 2-benzyl ester (8-2*S*). Compound **8**-2*S* was obtained in a similar manner to **8**-2*R*, described above.

4.3.13. (1*R*,2*R*,4*S*)-7-(Fluorenylmethyl)-7-azabicyclo[2.2.1]heptane-2,7-dicarboxylic acid (9-2*R*). Debenzylation of **8**-2*R* (400.0 mg, 0.88 mmol) was carried out by hydrogenation over Pd/C (94.7 mg) in MeOH (10 mL) at rt for 24 h. The reaction mixture was filtered and the filtrate was evaporated to give a crude oil, which was chromatographed (*n*-hexane/$CHCl_3$=1/6, then a small amount of acetic acid was added to the eluent) to give **9**-2*R* as a pale yellow oil (190 mg, 60% yield). Pale yellow amorphous solid. MS (*m*/*z*): 363 ($M+H^+$). HRMS (EI^+, $M+H^+$) calcd for $C_{22}H_{21}NO_4$: 363.1471; obsd: 363.1496. ^{1}H NMR: 7.78–7.76 (2H, m), 7.60–7.57 (2H, m), 7.42–7.38 (2H, m), 7.34–7.30 (2H, m), 4.49 (2H, d, J=6.2 Hz), 4.45 (1H, br s), 4.23 (1H, br s, overlap), 4.22 (1H, t, J=6.2 Hz), 2.93 (1H, br s), 1.95–1.45 (6H, m). $[\alpha]_D^{21}$ −14.4 (*c* 0.46, $CHCl_3$).

4.3.14. (1*S*,2*S*,4*R*)-7-(Fluorenylmethyl)-7-azabicyclo[2.2.1]heptane-2,7-dicarboxylic acid (9-2*S*). Compound **9**-2*S* was obtained in a similar manner to **9**-2*R*, described above. $[\alpha]_D^{21}$ +14.6 (*c* 0.48, $CHCl_3$).

4.3.15. Boc-(*S*-Ah2c)$_2$-OBn. Compound **7**-2*S* (252 mg, 0.76 mmol) was dissolved in 4 N HCl in dioxane (1.7 mL) and stirred for 1 h. The solvent was then removed in vacuum, and the residue was dried in vacuum. Compound **5**-2*S* (171 mg, 0.74 mmol) and DMAP (129.0 mg, 1.06 mmol) were added to the flask, followed by the addition of DMF (3 mL). Then EDCI·HCl (284 mg, 1.48 mmol) was added, and the whole was stirred for 48 h under Ar. DMF was removed in vacuum and the residue was washed with 1 N aqueous HCl, the whole was extracted with $CHCl_3$, then the solvent was evaporated to give a white sticky solid, which was chromatographed (*n*-hexane/AcOEt=1/1) to give a colorless amorphous solid (270 mg, 78% yield). MS (*m*/*z*): 455 ($M+H^+$). HRMS (FAB^+, $M+H^+$) calcd for $C_{26}H_{35}N_2O_5$: 455.2541; obsd: 455.2548. ^{1}H NMR: 7.38–7.35 (5H, m), 5.17–5.15 (2H, a mixture of conformers), (amide *cis*–*trans* mixture) 4.88 (0.5H, m), 4.67 (0.5H, m),

4.52 (0.5H, m), 4.35 (0.5H, m), 3.10–3.03 (2H, m), 2.08–1.50 (12H, m), 1.48 (9H, m).

4.3.16. HCl·H-(*S*-Ah2c)$_2$-OH. Debenzylation of Boc-(*S*-**Ah2c**)$_2$-OBn (77 mg, 0.17 mmol) was carried out by hydrogenation over Pd/C (60.1 mg) in MeOH (1.5 mL) at rt for 1.5 h. The reaction mixture was filtered and the filtrate was evaporated to give a crude oil. The residue was dissolved in 4 N HCl in dioxane (0.4 mL) and the resultant solution was stirred for 1 h. The solvent was then removed by a stream of Ar, and the residue was dried in vacuum to afford HCl·H-(*S*-**Ah2c**)$_2$-OH (63 mg, quant.). HRMS (FAB$^+$, M+H$^+$) calcd for $C_{14}H_{21}N_2O_3$: 265.1552; obsd: 265.1587.

4.3.17. HCl·H-(*S*-Ah2c)$_3$-OH. The preparation of HCl·H-(*S*-**Ah2c**)$_3$-OH was carried out in a similar manner to the dimer HCl·H-(*S*-**Ah2c**)$_2$-OH. HRMS (FAB$^+$, M+H$^+$) calcd for $C_{21}H_{30}N_3O_4$: 388.2236; obsd: 388.2207.

4.3.18. HCl·H-(*S*-Ah2c)$_4$-OH. The preparation of HCl·H-(*S*-**Ah2c**)$_4$-OH was carried out in a similar manner to the dimer HCl·H-(*S*-**Ah2c**)$_2$-OH. HRMS (FAB$^+$, M+H$^+$) calcd for $C_{28}H_{39}N_4O_5$: 511.2921; obsd: 511.2830.

4.3.19. HCl·H-(*S*-Ah2c)$_5$-OH. The preparation of HCl·H-(*S*-**Ah2c**)$_5$-OH was carried out in a similar manner to the dimer HCl·H-(*S*-**Ah2c**)$_2$-OH. HRMS (FAB$^+$, M+H$^+$) calcd for $C_{28}H_{39}N_4O_5$: 634.3605; obsd: 634.3559.

4.4. Solid-phase synthesis of Ah2c oligomers

4.4.1. Reversed-phase (RP) HPLC analysis and purification. RP-HPLC purification was performed on a Cosmosil 5C18-AR-II column (10×250 mm, Nacalai Tesque) with a linear gradient of A (0.1% TFA in H_2O) and B (0.1% TFA in MeCN) at a flow rate of 1 mL min^{-1} (Hitachi HPLC system); UV detection at 215 nm.

4.4.2. Peptide synthesis.

4.4.2.1. H-(*R*-Ah2c)$_8$-NH$_2$. The Rink amide resin (200 mg, 0.04 mmol; loading 0.21 mmol g^{-1}) was swelled in DMF (5 mL) for 90 min and Fmoc was deprotected using 20% piperidine in DMF (2 mL, 15 min). The resin was filtered and washed with DMF (5×4 mL). A solution of Fmoc-*R*-**Ah2c**-OH (**9**-2*R*) (43 mg, 3 equiv), PyBOP (3 equiv) and HOBt (3 equiv) in DMF (0.9 mL), and *N*-methylmorpholine (6 equiv) were added successively to the resin and the suspension was mixed for 1.5 h at rt. The resin was then filtered and washed with DMF (5×4 mL) prior to the following Fmoc deprotection step. The Fmoc group was removed using 20% piperidine in DMF (2 mL, 15 min). The resin was filtered and washed with DMF (5×4 mL). For each coupling, a solution of the Fmoc-amino acid (3 equiv), PyBOP (3 equiv) and HOBt (3 equiv) in DMF (0.9 mL), and *N*-methylmorpholine (6 equiv) were added successively to the resin and the suspension was mixed for 1.5 h at rt. The resin was then filtered and washed with DMF (5×4 mL). After coupling the last amino acid, the Fmoc group was cleaved and the resin was washed with DMF (5×4 mL), MeOH (5×4 mL), Et_2O (5×4 mL). Drying overnight under vacuum afforded the Fmoc-deprotected peptide-resin (209 mg). The dry Fmoc-deprotected peptide-resin was treated with a mixture of TFA (10 mL) and ethanedithiol (0.5 mL) for 2 h at rt. The resin was filtered and the reaction mixture was evaporated. The precipitate formed upon addition of cold Et_2O (15 mL) to the oily residue was separated by decanting the solvent. The precipitate was lyophilized to yield 25 mg of the crude peptide. Purification of the crude peptide by RP-HPLC (15–40% B in 25 min) afforded the TFA salt of H-(*R*-**Ah2c**)$_8$-NH$_2$, 4.91 mg (4.1%) as a white fluffy powder. MS (*m*/*z*): 1003.75 (M+H$^+$). MS (*m*/*z*) (ESI$^+$, [M+H]$^+$) calcd for $C_{56}H_{76}N_9O_8$: 1002.5811; obsd: 1002.5804.

4.4.2.2. H-(*S*-Ah2c)$_4$-NH$_2$. The preparation of H-(*S*-**Ah2c**)$_4$-NH$_2$ was carried out in a similar manner to (*R*-**Ah2c**)$_8$-NH$_2$. Colorless oil. MS (*m*/*z*): 511 (MALDI-TOF MS, [M+H]$^+$).

4.4.2.3. H-(*S*-Ah2c)$_5$-NH$_2$. The preparation of H-(*S*-**Ah2c**)$_5$-NH$_2$ was carried out in a similar manner to H-(*R*-**Ah2c**)$_8$-NH$_2$. Colorless oil. MS (*m*/*z*): 633 (MALDI-TOF MS, [M+H]$^+$).

4.4.2.4. H-(*S*-Ah2c)$_8$-NH$_2$. The preparation of H-(*S*-**Ah2c**)$_8$-NH$_2$ was carried out in a similar manner to H-(*R*-**Ah2c**)$_8$-NH$_2$. White fluffy powder. MS (*m*/*z*) (ESI-TOF, [M+H]$^+$) calcd for $C_{56}H_{76}N_9O_8$: 1002.5811; obsd: 1002.5770.

4.5. CD measurements

Dry peptide samples were weighed and dissolved in an appropriate amount of spectroscopic grade methanol. Sample cells of 1-mm path length were used. Data were collected on a JASCO J-820 spectrometer at 20 °C. Data are represented in terms of mean residue ellipticity, [θ] (deg cm^2 decimol^{-1} residue^{-1}).

The mean residue ellipticities for H-(*S*-**Ah2c**)$_8$-NH$_2$ are ca. -3.5×10^4 deg cm^2 decimol^{-1} residue^{-1} at 198 nm (a minimum) and 4.0×10^4 at 217 nm (a maximum), while those for H-(*R*-**Ah2c**)$_8$-NH$_2$ are 4.0×10^4 at 198 nm and -3.1×10^4 at 217 nm. The two oligomers have the crossover point at about 206 nm.

The positions and intensities of the minimum and maximum peaks of H-(*S*-**Ah2c**)$_4$-NH$_2$ and HCl·H-(*S*-**Ah2c**)$_4$-OH in the CD spectra are practically identical, H-(*S*-**Ah2c**)$_4$-NH$_2$: ca. -1.9×10^4 deg cm^2 decimol^{-1} residue^{-1} at 197 nm (minimum) and 2.4×10^4 at 216 nm (maximum); HCl·H-(*S*-**Ah2c**)$_4$-OH: ca. -2.0×10^4 deg cm^2 decimol^{-1} residue^{-1} at 197 nm (minimum) and 2.4×10^4 at 216 nm (maximum).

Acknowledgements

This work was supported by a Grant-in-Aid for Scientific Research (Category S, No. 17109001) to T.O., and in part by a Grant-in-Aid (No. 17350063) for Scientific Research and the COE project, Giant Molecules and Complex Systems 2005, from the Ministry of Education, Science, Sports, Culture, and Technology to N.K. A part of the calculations was carried out at the Computer Center of the Institute for Molecular Science and the Computer Center of the University of Tokyo. We thank these computational facilities for

generous allotments of computer time. We also thank Masatoshi Kawahata for assistance in crystal structure analysis.

Supplementary data

Supporting information, additional structural data, and ^{1}H NMR spectra are available. Supplementary data associated with this article can be found in the online version, at doi:10.1016/j.tet.2006.09.062.

References and notes

1. (a) Seebach, D.; Abele, S.; Gademann, K.; Guichard, G.; Hintermann, T.; Jaun, B.; Matthews, J. L.; Schreiber, J. V.; Oberer, L.; Hommel, U.; Widmer, H. *Helv. Chim. Acta* **1998**, *81*, 932–982; (b) Review: Seebach, D.; Matthews, J. *Chem. Commun.* **1997**, 2015–2022; (c) Seebach, D.; Beck, A. K.; Bierbaum, D. J. *Chem. Biodivers.* **2004**, *1*, 1111–1239.
2. Review: (a) Cheng, R. P.; Gellman, S. H.; DeGrado, W. F. *Chem. Rev.* **2001**, *101*, 3219–3232; (b) Appella, D. H.; Christianson, L. A.; Klein, D. A.; Powell, D. R.; Huang, X.; Barchi, J. J., Jr.; Gellman, S. H. *Nature* **1997**, *387*, 381–384; (c) Appella, D. H.; Barchi, J. J.; Durell, S. R.; Gellman, S. M. *J. Am. Chem. Soc.* **1999**, *121*, 2309–2310; (d) While β-proline oligomers form helices without intramolecular hydrogen bonding, their amide bonds are planar; the sum of the bond angles around the amide nitrogen is 359.95° in the crystal structure of the dimers of β-proline derivatives: Huck, B. R.; Fisk, J. D.; Guzei, I. A.; Carlson, H. A.; Gellman, S. H. *J. Am. Chem. Soc.* **2003**, *125*, 9035–9037; (e) Schmitt, M. A.; Weisblum, B.; Gellman, S. H. *J. Am. Chem. Soc.* **2004**, *126*, 6848–6849.
3. (a) Seebach, D.; Albert, M.; Arvidsson, P. I.; Rueping, M.; Schreiber, J. V. *Chimia* **2001**, *55*, 345–353; (b) Hamuro, Y.; Schneider, J. P.; DeGrado, W. F. *J. Am. Chem. Soc.* **1999**, *121*, 12200–12201; (c) Porter, E. A.; Wang, X.; Lee, H.-S.; Weisblumand, B.; Gellman, S. H. *Nature* **2000**, *404*, 565.
4. For a review of foldamers: Hill, D. J.; Mio, M. J.; Prince, R. B.; Hughes, T. S.; Moore, J. S. *Chem. Rev.* **2001**, *101*, 3893–4011.
5. (a) Ohwada, T.; Achiwa, T.; Okamoto, I.; Shudo, K. *Tetrahedron Lett.* **1998**, *39*, 865–868; (b) Review: Ohwada, T. *Yakugaku Zasshi* **2001**, *121*, 65–77; (c) Otani, Y.; Nagae, O.; Naruse, Y.; Inagaki, S.; Ohno, M.; Yamaguchi, K.; Yamamoto, G.; Uchiyama, M.; Ohwada, T. *J. Am. Chem. Soc.* **2003**, *125*, 15191–15199.
6. Non-planarity of peptide bonds has been discussed: (a) Winkler, F. K.; Dunitz, J. D. *J. Mol. Biol.* **1971**, *59*, 169–182; (b) Buck, M.; Karplus, M. *J. Am. Chem. Soc.* **1999**, *121*, 9645–9658; (c) Mannfors, B. E.; Mirkin, N. G.; Palmo, K.; Krimm, S. *J. Phys. Chem. A* **2003**, *107*, 1825–1832; (d) Fischer, S.; Dunbrack, R. L.; Karplus, M. *J. Am. Chem. Soc.* **1994**, *116*, 11931–11937; (e) Head-Gordon, T.; Head-Gordon, M.; Frisch, M. J.; Brooks, C. L., III; Pople, J. *J. Am. Chem. Soc.* **1991**, *113*, 5989–5997; (f) Guo, H.; Karplus, M. *J. Phys. Chem.* **1992**, *96*, 7273–7287; (g) Sulzbach, H. M.; Schleyer, P. v. R.; Schefer, H. F., III. *J. Am. Chem. Soc.* **1995**, *117*, 2632–2637; (h) MacArthur, M. W.; Thornton, J. M. *J. Mol. Biol.* **1996**, *264*, 1180–1195; (i) Hu, J.-S.; Bax, A. *J. Am. Chem. Soc.* **1997**, *119*, 6360–6368.
7. An example of the use of the present bicyclic structure as a peptidomimetic was presented by Avenoza, A.; Busto, J. H.; Peregrina, J. M.; Rodriguez, F. *J. Org. Chem.* **2002**, *67*, 4241–4249.
8. Zhang, C.; Trudell, M. L. *J. Org. Chem.* **1996**, *61*, 7189–7191.
9. The structure of 7-(*tert*-butoxycarbonyl)-2-*endo*-bornane-2,10-sultam-7-azabicyclo[2.2.1]heptane (**6b**) was determined by X-ray crystallographic analysis.
10. This kind of molecular weight dependence of the CD spectra is one of the criteria for judging the helical nature of polymers (Gu, H.; Nakamura, Y.; Sato, T.; Teramoto, A.; Green, M. M.; Andreola, C.; Peterson, N. C.; Lifson, S. *Macromolecules* **1995**, *28*, 1016–1024); and oligomers (Stone, M. T.; Heemstra, J. M.; Moore, J. S. *Acc. Chem. Res.* **2006**, *39*, 11–20).
11. (a) Mitaku, S.; Suzuki, K.; Odashima, S.; Ikuta, K.; Suwa, M.; Kukita, F.; Ishikawa, M.; Itoh, H. *Proteins* **1995**, *22*, 350–362; (b) Bhakuni, V. *Arch. Biochem. Biophys.* **1998**, *357*, 274–284.
12. A similar intra-residue attraction was discussed in Tanatani, A.; Yokoyama, A.; Azumaya, I.; Takakura, Y.; Mitsui, C.; Shiro, M.; Uchiyama, M.; Muranaka, A.; Kobayashi, N.; Yokozawa, T. *J. Am. Chem. Soc.* **2005**, *127*, 8553–8561.
13. Berova, N.; Nakanishi, K.; Woody, R. W. *Circular Dichroism: Principles and Applications*, 2nd ed.; Wiley-VCH: New York, NY, 2000.
14. (a) Browett, W. R.; Stillman, M. J. *Comput. Chem.* **1987**, *11*, 241–250; (b) Gasyna, Z.; Browett, W. R.; Nyokong, T.; Kitchenham, R.; Stillman, M. J. *Chemom. Intell. Lab. Syst.* **1989**, *5*, 233–246; (c) Mack, J.; Stillman, M. J. *Handbook of Porphyrins and Related Macrocycles*; Kadish, K., Smith, K., Guilard, R., Eds.; Academic: New York, NY, 2003; Vol. 16, Chapter 103, pp 43–116.
15. Schellman, J. A.; Oriel, P. J. *J. Chem. Phys.* **1962**, *37*, 2114–2124.
16. Moffitt, W.; Fitts, D. D.; Kirkwood, J. G. *Proc. Natl. Acad. Sci. U.S.A.* **1957**, *43*, 723–730.
17. Sandvoss, L. M.; Carlson, H. A. *J. Am. Chem. Soc.* **2003**, *125*, 15855–15862.
18. Leroy, J. *Synth. Commun.* **1992**, *22*, 567–572.
19. Singh, S.; Basmadjian, G. P. *Tetrahedron Lett.* **1997**, *38*, 6829–6830.
20. Hern′andez, A.; Macros, M.; Rapoport, H. *J. Org. Chem.* **1995**, *60*, 2683–2691.